



OPEN

SUBJECT AREAS:
LIGHT RESPONSES
PLANT BREEDING

Received
25 April 2014

Accepted
8 December 2014

Published
9 January 2015

Correspondence and
requests for materials
should be addressed to
H.S. (sh6117@kais.
kyoto-u.ac.jp)

* These authors
contributed equally to
this work.

The effects of phytochrome-mediated light signals on the developmental acquisition of photoperiod sensitivity in rice

Yoshihiro Yoshitake^{1*}, Takayuki Yokoo^{1*}, Hiroki Saito¹, Takuji Tsukiyama¹, Xu Quan¹, Kazunori Zikihara², Hitomi Katsura², Satoru Tokutomi², Takako Aboshi³, Naoki Mori³, Hiromo Inoue¹, Hidetaka Nishida⁴, Takayuki Kohchi⁵, Masayoshi Teraishi¹, Yutaka Okumoto¹ & Takatoshi Tanisaka^{1,6}

¹Division of Agronomy and Horticulture Science, Graduate School of Agriculture, Kyoto University, Sakyo, Kyoto 606-8502, Japan,

²Department of Biological Science, Graduate School of Science, Osaka Prefecture University, Sakai, Osaka 599-8531, Japan,

³Division of Applied Life Sciences, Graduate School of Agriculture, Kyoto University, Sakyo, Kyoto 606-8502, Japan, ⁴Graduate School of Environmental and Life Science, Okayama University, Okayama 700-8530, Japan, ⁵Graduate School of Biostudies, Kyoto University, Sakyo, Kyoto 606-8502, Japan, ⁶Department of Agricultural Regional Vitalization, Kibi International University, Minamiawaji, Hyogo, 656-0484, Japan.

Plants commonly rely on photoperiodism to control flowering time. Rice development before floral initiation is divided into two successive phases: the basic vegetative growth phase (BVP, photoperiod-insensitive phase) and the photoperiod-sensitive phase (PSP). The mechanism responsible for the transition of rice plants into their photoperiod-sensitive state remains elusive. Here, we show that *se13*, a mutation detected in the extremely early flowering mutant X61 is a nonsense mutant gene of *OsHY2*, which encodes phytochromobilin (PΦB) synthase, as evidenced by spectrometric and photomorphogenic analyses. We demonstrated that some flowering time and circadian clock genes harbor different expression profiles in BVP as opposed to PSP, and that this phenomenon is chiefly caused by different phytochrome-mediated light signal requirements: in BVP, phytochrome-mediated light signals directly suppress *Ehd2*, while in PSP, phytochrome-mediated light signals activate *Hd1* and *Ghd7* expression through the circadian clock genes' expression. These findings indicate that light receptivity through the phytochromes is different between two distinct developmental phases corresponding to the BVP and PSP in the rice flowering process. Our results suggest that these differences might be involved in the acquisition of photoperiod sensitivity in rice.

Flowering time plays a principal role in the regional adaptability of plants. In rice (*Oryza sativa* L.), a facultative short-day plant, flowering time is promoted under short-day length (SD), but is delayed under long-day length (LD). Development before floral initiation in rice is divided into two phases: the basic vegetative growth phase (BVP) and the photoperiod sensitive phase (PSP), and different rice varieties vary widely in the durations of the two phases^{1,2}. During BVP, even varieties with strong photoperiod sensitivities do not respond to daylength^{1,2}.

To date, several flowering time genes have been identified. Among these, *Heading date 3a* (*Hd3a*) and *RICE FLOWERING LOCUS T 1* (*RFT1*), two orthologs of *Arabidopsis FLOWERING LOCUS T* (*FT*) that are known as florigen-like genes, are expressed in the vascular tissues, and their proteins of leaves move to the shoot apical meristem (SAM) through the phloem^{3–5}. Upstream of *Hd3a* and *RFT1*, *Heading date 1* (*Hd1*) and *Early heading date 1* (*Ehd1*), two major floral signal integrators, process multiple signals^{6,7} originating from *OsMADS50*⁸, *OsMADS51*⁹, *OsMADS56*¹⁰, *Grain number, plant height, and heading date 7* (*Ghd7*)¹¹, *Ehd3*¹², *OsCOL4*¹³, *Os-GIGANTEA* (*OsGI*, an ortholog of *Arabidopsis GIGANTEA* [*GI*])^{14,15}, *Ehd2* (an ortholog of maize *INDETERMINATE 1* [*ID1*], and also known as *RID1* and *OsID1*)^{16–18} and *Hd6*¹⁹. *Hd1* and *Ehd1* are activated by *OsGI* and *Ehd2*, respectively^{14,16}. In contrast, the expression of *Ghd7*, which encodes a CO, CO-LIKE, and TIMING OF CAB1 (CCT) motif-containing protein, is specifically upregulated in response to long-day (LD) conditions to repress *Ehd1* expression¹¹. The expression level of *Ghd7* is determined by the coincidence of the



timing of gating and phytochrome-mediated light signals²⁰. Although many genetic factors that control flowering time in rice so far have been identified already, it remains unknown how rice developmentally acquires photoperiod sensitivity.

Recent studies in *Arabidopsis thaliana*, a long day model plant, have demonstrated the participation of a circadian clock in photoperiodic control of flowering time and have shown that its molecular base is composed of three major loops. This series of interlocked transcription–translation feedback loops constitutes the regulatory network of the circadian clock. The first loop is composed of the pseudo response regulator *TIMING OF CAB EXPRESSION 1 (TOC1)*²¹ and two partially redundant *Myb*-like transcription factors, *LATE ELONGATED HYPOCOTYL (LHY)*²² and *CIRCADIAN CLOCK ASSOCIATED 1 (CCA1)*²³. In the morning, expression of *LHY* and *CCA1* represses *TOC1* by binding to its promoter²⁴. The circadian accumulation of *TOC1* in the evening then induces expression of *LHY* and *CCA1*. In the morning, the accumulation of *LHY* and *CCA1* also activates two *TOC1*-related protein genes, *PSEUDO RESPONSE REGULATOR 7 (PRR7)* and *PRR9*^{25,26}, which subsequently repress *LHY* and *CCA1*. In the evening, *GI* activates *TOC1* expression, but in turn is negatively regulated by *LHY*, *CCA1* and *TOC1*^{27,28}. In rice, several clock-related genes have been identified based on daily amplitude rhythms and homology searches, including *OsLHY*, *OsPRR1*, *OsPRR37* (also known as *Hd2*), *OsPRR73*, *OsPRR59*, and *OsPRR95*^{29–31}. In addition, the flowering time genes of *OsGI* and *Ef7* (also known as *Hd17* and *OsELF3-1*) have also been identified as clock-related genes^{15,16,32–35}.

It has recently been reported that the amplitudes of clock gene expressions are significantly reduced in the *Arabidopsis* phytochrome null mutant (*phyABCDE*)³⁶. It has also been reported that the cooperative interaction between the clock-related gene *EARLY FLOWERING 3 (ELF3)* and *Phytochrome* genes contribute to the maintenance of the clock gene expressions³⁷. These findings indicate that the phytochrome-mediated light signals play critical roles in the maintenance of clock oscillation and amplitude in *Arabidopsis*. On the other hand, only three relevant molecules have been identified in the rice genome: *PhyA*, *PhyB*, and *PhyC*. The triple mutant *phyABC* exhibits significantly reduced photoperiod sensitivity³⁸. Additionally, the loss of function mutant of the rice *Se5* gene, an ortholog of the *Arabidopsis HY1* gene, which encodes heme oxygenase that converts heme to biliverdin IX α (BV) in the phytochrome-chromophore biosynthesis pathway, eliminates photoperiod sensitivity due to the complete deficiency of phytochromobilin (P Φ B) synthesis that is essential for photo-interconversion between Pr and Pfr^{39,40}. Phytochromes and phytochrome-chromophore are thus significantly involved in photoperiod sensitivity in rice. Little is known, however, about the developmental stage-dependent effect of phytochrome-mediated light signaling on the oscillation of circadian clock genes in rice.

Our previous study indicated that the extremely early flowering of the mutant line X61 was caused by a complete loss of photoperiodic response due to a novel single recessive mutant gene, *se13*. Since X61 harbored a 1-bp insertion in exon 1 of *OsHY2*, we assumed that *se13* is a mutant gene of *OsHY2*, encoding P Φ B synthase, which is involved in the final step in the phytochrome-chromophore biosynthesis pathway⁴¹. In that study, however, we were able to demonstrate only a strong possibility that the *Se13* locus is identical to the *OsHY2* locus based on linkage and subsequent sequence analysis. In this study, we verified that *se13* in X61 is a nonsense mutant gene of *OsHY2* by conducting a complementation test and phytochrome spectrum analysis, and that X61 and two *Se13*-silenced lines exhibit repressed photo-morphogenesis caused by blinding of the red/far-red light signals. Subsequent expression analysis showed that the expression profiles of a few flowering time genes are influenced by the genotype at the *Se13* locus on one level or another and differ between the BVP stage and the primary stage of PSP. These findings

indicate that light receptivity through the phytochromes is different between two distinct developmental phases corresponding to the BVP and PSP in the rice flowering process.

Results

The *Se13* gene is identical to the *OsHY2* gene. X61 harbors a single base insertion (C) in exon 1 of *OsHY2*⁴¹, which exhibits 49% similarity to *HY2* in *Arabidopsis*. We first conducted a complementation test of *se13* to ascertain whether the *Se13* locus is identical to the *OsHY2* locus. Before the complementation test, we carried out a 3'-RACE (rapid amplification of cDNA ends) PCR for the *Se13* transcripts and identified six different RACE products (Supplementary Fig. S1a and b). Using the ORF finder (NCBI; <http://www.ncbi.nlm.nih.gov/projects/gorf/>), we predicted their coding sequences to specify the single RACE fragment encoding the putative *Se13* cDNA fragment of 906 bp (~34 kDa) length. We introduced this 906-bp cDNA into X61 under the control of a CaMV 35S promoter. The *Agrobacterium*-mediated gene transformation was conducted according to a procedure⁴² optimized for the “Gimbozu” variety (WT). We tested the flowering time of two independently obtained transgenic plants (X61^{Comp.} #1, #2) under a 14.5-h daylength (LD) and a 10-h daylength (SD). Consequently, the cDNA fragment (35S::*Se13*) from WT fully rescued the photoperiod-insensitive phenotype of the transgenic plants under LD conditions (Fig. 1a–c). In *Arabidopsis*, *HY2* is a downstream gene of *HY1* in the phytochrome-chromophore biosynthesis pathway^{43,44}. In rice, *Se5* has been shown to be an ortholog of *HY1*³⁹. Knowing this, we checked the flowering time of an *Se5*-deficient mutant (*se5Se13*) and a double mutant (*se5se13*); we found that both mutants flowered at the same time as did *se13* mutant (*Se5se13*), under not only SD but also LD conditions (Supplementary Fig. S2). These results indicate that *Se13* is a downstream gene of *Se5*. Next, we measured spectrophotometrically detectable phytochrome⁴⁵ in X61 to see if *se13* affects its concentration. In WT, crude extracts from etiolated seedlings exhibited a typical red/far-red reversible spectrum of phytochrome A. In X61 under the same conditions, the phytochrome signal was undetectable (Fig. 1d, left). When the extract was prepared from a 10-fold larger quantity of tissues, however, a small signal was observed (Fig. 1d, right).

Taking these findings together with the results of the complementation test and the red and far-red light response test, we concluded that the *Se13* locus is identical to *OsHY2*, which is similar to *Arabidopsis HY2*, which encodes P Φ B synthase, and *se13* of X61 is a leaky mutant allele that retains a weak ability to respond to red and far-red light.

Molecular characterization of *Se13*. In order to further characterize the *Se13* gene, we produced *Se13*-silenced plants with an RNAi-silencing vector PANDA⁴⁶. The effects of *Se13*-silencing were evaluated using two *T*₁ lines derived from two independently obtained *T*₀ plants that were heterozygous for the transgene (*Se13*-silenced gene). The expression of *Se13* was strongly silenced in the two *T*₁ lines (*Se13-RNAi* #1, *Se13-RNAi* #3) as compared to WT (Fig. 2b). Subsequently, we investigated the effects of light and dark conditions on the seedling growth of *Se13-RNAi* #1, #3, X61, and WT (Fig. 2a, d). In the dark, all lines exhibited elongated coleoptiles and third leaves (Fig. 2a, d). In white light, seedling elongation was not inhibited in *Se13-RNAi* lines, but was inhibited in X61 and WT. In third leaf length and coleoptile length, significant differences were observed among the lines (Fig. 2d): third leaf lengths in *Se13-RNAi* #1, #3, X61, and WT were 14.8 ± 1.96 cm, 14.2 ± 2.10 cm, 12.5 ± 1.05 cm, and 10.06 ± 1.271 cm, respectively, and coleoptile lengths in *Se13-RNAi* #1, #3, X61, and WT were 0.96 ± 0.09 cm, 0.91 ± 0.12 cm, 0.93 ± 0.1 cm, and 0.44 ± 0.05 cm, respectively. Thus, the degree of light inhibition in X61 was

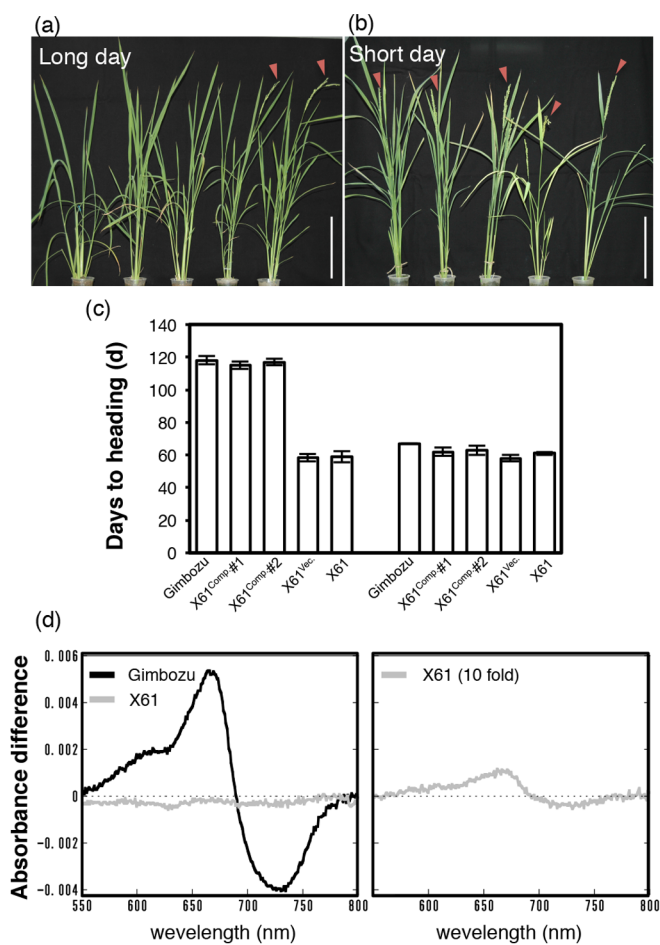


Figure 1 | *Se13* encodes the phytochromobilin synthase in rice. (a–e) *se13* mutant fully rescued the photoperiod-insensitive phenotype in the transgenic plants as shown through complementation test. (a, b) Plants grown under LD (a) and SD (b) conditions are shown from left to right: Gimbozu (WT), T₂ lines complemented with the *Se13* coding sequence (X61^{Comp}) #1, #2, vector control (X61^{Vec}) and X61 (*se13*). Arrowheads indicate panicle heads, scale, 20 cm. (c) Flowering times are shown as days to heading under LD (left side) and SD (right side) conditions. Average values \pm s.d. (standard deviation) are shown ($n = 10$). (d) Spectra for photoreversible phytochromes Left, absorption difference spectra of the partially purified extract of 10-day-old dark-grown shoots of WT (black line) and X61 (grey line). Right, 10-fold concentrated extract of X61.

intermediate between that in the *Se13*-RNAi and that in WT, supporting the earlier finding that *se13* in X61 is a leaky mutant gene.

Interestingly, at the three-leaf stage, the growth of T₁ seedlings homozygous for the transgene was arrested; their leaves turned white and blighted, and eventually withered. It has been demonstrated previously that rice has only three different phytochrome genes (*phyA-C*) serving as red/far-red light receptors³⁸, and that mutations in the phytochrome-chromophore biosynthesis pathway affect all phytochrome species. On the other hand, phytochrome deficiency itself does not induce a lethal phenotype; the *phyABC* triple mutants and the *se5* (*oshy1*) mutant, in which the chromophore biosynthesis pathway is blocked by loss-of-function of *Se5* (*OshY1*), continue to grow until flowering^{39,40}. To determine the mechanistic relationship between the loss-of-function of the *Se13* (*OshY2*) gene and the termination of rice growth at the three-leaf stage, we examined the chlorophyll contents of *Se13*-RNAi #1, #3, X61, and WT. We further measured the contents of three precursors in the tetrapyrrole pathway, protoporphyrin IX (Proto), Mg-protoporphyrin IX (Mg-Proto), and Mg-protoporphyrin monomethyl ester (Mg-ProtoMe)

(Fig. 2c). The chlorophyll *a* and *b* contents in *Se13*-RNAi #1 and #3 were significantly lower than those in X61 and WT (Fig. 2e). No significant differences in chlorophyll *a* and *b* contents between X61 and WT were observed, although X61 showed slightly lower levels than WT. In contrast, the contents of Mg-Proto and Mg-ProtoMe, both of which are metabolites in the chlorophyll biosynthetic pathway, did not significantly differ among the four lines. Compared to WT, however, *Se13*-RNAi #1, #3, and X61 accumulated abundant Proto (Fig. 2f).

Analysis of the effect of *se13* on the duration of BVP. To estimate the transition day from BVP to PSP in X61 and wild-type (WT), we conducted a photoperiod transfer treatment, starting with a long daylength (LD; 24-h) and shifting to a short daylength (SD; 10-h) according to the model of Ellis et al.⁴⁷ with slight modifications^{2,32}. In the transfer treatments, 13 pots for each line were initially kept under a 24-h daylength. The days to flowering of both X61 and WT were constant in plants that had been transferred early, but gradually increased with the length of time that had passed before the transfer. Using this analytical model, we successfully estimated the duration of BVP and the degree of PS expressed by regression coefficient (*b*) of days to flowering on transfer time during PSP under SD conditions (Fig. 3a). First, we started the photoperiodic transfer treatment with a 14.5-h daylength to create LD conditions. The duration of BVP in WT was calculated at 22.69 days. We could not calculate the duration of BVP in X61, because we could not identify the transition day of X61 from BVP to PSP due to its extremely weak photoperiod sensitivity (Supplementary Fig. S3). Under 24-h daylength conditions, however, we did observe that the flowering time of X61 was slightly delayed (Supplementary Fig. S4), confirming that X61 has extremely weak photoperiod sensitivity. Thus, we were able to estimate the transition day of X61 based on its behavior under 24-h daylength conditions. The BVP durations of X61 and WT were thus estimated at 23.7 ± 1.01 and 23.2 ± 0.87 days, respectively (Fig. 3b and c). The mutant allele *se13* was found not to affect the duration of BVP at all, and the transition from BVP to PSP occurs just after 23 or 24 days after sowing (DAS). X61 exhibited a far smaller *b* value (0.346) than WT (0.934). Since *b* is an index of photoperiod sensitivity, this implies that *se13* almost, but not completely, excludes photoperiod sensitivity.

Effect of *se13* on the expression of other flowering time-related genes. We examined the expression levels of flowering time and clock-related genes in X61 and WT to identify potential downstream genes regulated by *Se13* under LD conditions (14.5 h) at four different time points during development, 18, 22, 25 and 28 days after sowing (DAS). Based on the results of the photoperiod transfer treatment, we regarded the first two time points, at 18 and 22 DAS, as falling within of BVP, and the second two time points, at 25 and 28 DAS, as falling within the primary stage of early PSP (a few days after the termination of BVP). To identify developmental changes in the expression patterns of various genes related to the genotype at the *Se13* locus, we measured the expression levels at these four time points. The genes tested are listed in Supplementary Table 1.

We first investigated the expression levels of *Hd3a* and *RFT1*, both of which encode the mobile flowering signal florigen^{5,48}. At 18 DAS, *RFT1* and *Hd3a* exhibited a significantly higher expression level in X61 than in WT in the daytime, whereas at 22 DAS *Hd3a* exhibited a very low expression level in both X61 and WT, although *RFT1* still exhibited higher expression (Fig. 4a and b). Because *se13* of X61 is a leaky mutant, the repressions of *Hd3a* at 22 DAS in X61 might be attributed to the weak ability to respond to red and far-red light. Therefore, *RFT1* appeared to be solely responsible for promoting floral initiation in X61 under LD (Fig. 4a and b). Because *Ehd1* was also upregulated only in X61 in the daytime, it was evident that *Ehd1* promoted the expression of *RFT1* in X61. We also examined the

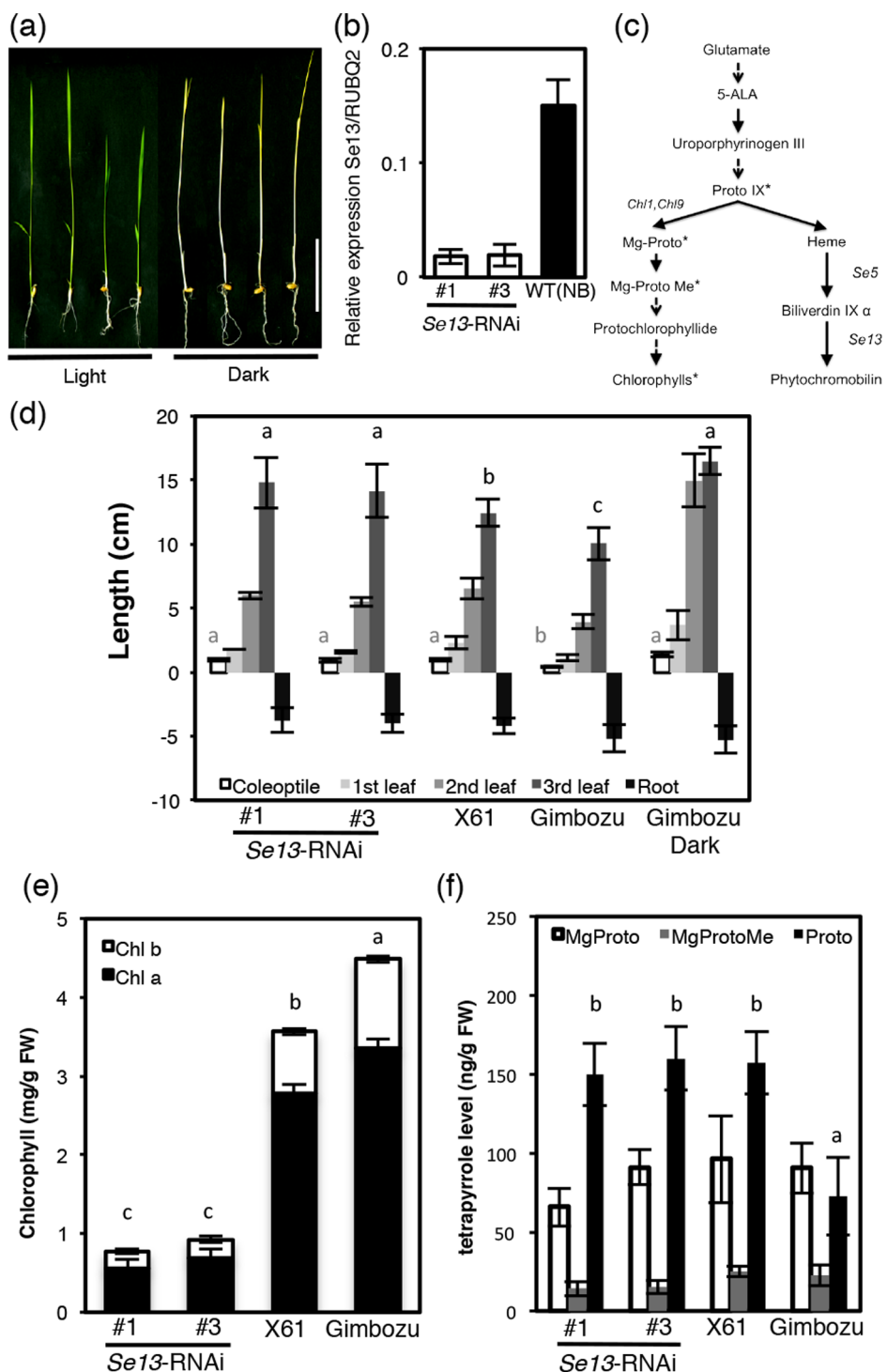


Figure 2 | Molecular characterization of *se13* plants. (a) Phenotypes of *Se13*-RNAi lines (#1, #3), X61, and WT (Nipponbare, NB) (from left to right). Plants were photographed at 12 days after sowing (DAS) under light (10 light/14 dark) and dark conditions. Scale, 5 cm (b) Expression levels of *Se13* transcripts in WT (NB) and *Se13*-RNAi plants. Samples were harvested from the second leaf blades of seedlings 12 DAS at ZT 9. Means \pm s.d. are shown ($n = 10$) (c) A schematic illustration of the metabolic pathway of tetrapyrrole adapted from previous reports^{39,51,68,69}. Abbreviations used are as follows: ProtoIX for protoporphyrin IX, Mg-Proto for Mg-protoporphyrin IX, Mg-ProtoMe for Mg-protoporphyrin monomethyl ester, Se5 for heme oxygenase 1, Se13 for phytochromobilin synthase, Chl1 for Mg-chelatase subunit D, and Chl9 for Mg-chelatase subunit I. Asterisks indicate quantified tetrapyrrole intermediates in this study. (d) Lengths of coleoptile and the third leaves of seedlings 12 DAS under light (10 light/14 dark) conditions. *Se13*-RNAi #1, #3, X61, and WT are represented in Figure 3d. (e) Chlorophyll content of *Se13*-RNAi #1, #3, X61 and WT. Means \pm s.d. are shown ($n = 10$). (f) Tetrapyrrole intermediates content of *Se13*-RNAi #1, #3, X61 and WT. Means \pm s.d. are shown ($n = 10$). Means followed by different letters are significantly different from that of WT [$P < 0.05$ according to Tukey's honest significant difference test (a, b or a–c)].

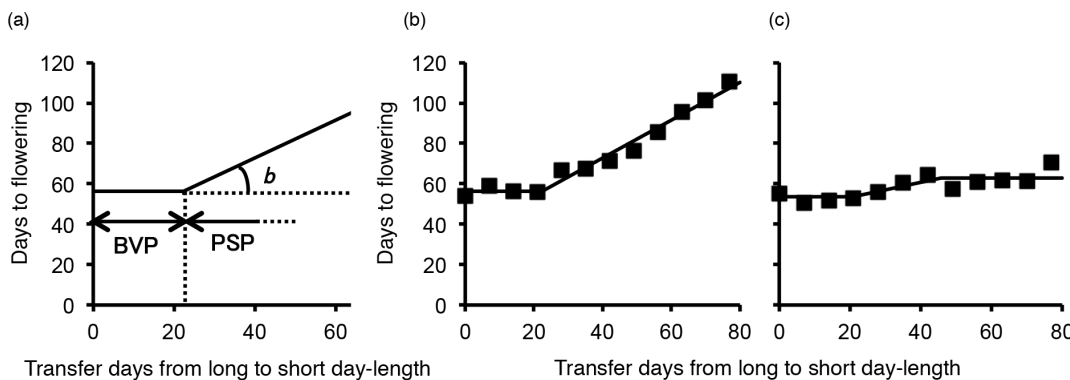


Figure 3 | Flowering responses of Gimbozu (WT) and X61 to the photoperiodic transfer treatment from long to short daylength. (a) Schematic representation of flowering responses of the plants transferred from long daylength to short daylength at various times after sowing. The double-headed arrow indicates the duration of the basic vegetative phase (BVP). *b* indicates the regression coefficient of days to flowering during photoperiod sensitive phase (PSP) on transfer days from long to short daylength. (b) Flowering response of Gimbozu (WT) (c) Flowering response of X61.

expression levels of the genes upstream of *Ehd1*, viz. *Ehd2* (also known as *RID1* and *OsID1*)^{16–18}, *Ehd3*¹², *OsMADS50*⁸, *OsMADS51*⁹, *OsMADS56*¹⁰, and *OsCOL4*¹³. Among these genes, *Ehd2* was specifically upregulated in X61, whereas the other genes exhibited no differences between X61 and WT (Fig. 4a and b, Supplementary Fig. S5). Furthermore, *Hd1* and *Ghd7*, which are key genes inhibiting the flowering pathway under non-inductive LD, were expressed in both X61 and WT, and the diurnal expression patterns and levels of these two genes were not affected by the genotype at the *Se13* locus (Fig. 4a and b). Interestingly, the expression of *Ghd7* at 22 DAS was higher than that at 18 DAS without any differences between X61 and WT (Fig. 4a and b). In addition, all other genes not previously described maintained their expression patterns and levels regardless of the genotype at the *Se13* locus (Supplementary Fig. S5). The results of this experiment thus indicate that *Se13* repressed the *Ehd1*-dependent flowering pathway by downregulating the *Ehd2* expression level under LD at 18 and 22 DAS, regardless of the high expressions of *Hd1* and *Ghd7* genes.

At 25 and 28 DAS, *Hd3a* was not upregulated in either X61 or WT, and the upregulation of *RFT1* was again observed only in X61 (Fig. 4c and d). Although *Ehd1* was also upregulated in X61, the expression of *Ehd2* was not changed compared to that in WT during the daytime. On the other hand, reductions in the expression of *Ghd7* were observed in X61 at both time points (Fig. 4c and d). Therefore, the upregulation of *Ehd1* in X61 was attributed to the reduced expression of *Ghd7* in addition to the lack of the modification of *Ghd7* protein by phytochrome due to the weak ability of X61 to synthesize phytochromobilin during this period. In addition to *Ghd7*, the expression level of *Hd1* in X61 during the daytime was reduced at 25 and 28 DAS, in contrast to 18 and 22 DAS (Fig. 4c and d). To understand the effects of *Se13* on the upstream genes of *Hd1*, we examined the expression levels of *OsGI*, *OsPRRI*, *OsPRR37* (*Hd2*), *OsPRR73*, *OsPRR59*, and *OsPRR95*. In X61, the peak expression levels of *OsGI* and most of the *OsPRR* gene series were lower than those in WT (Fig. 5 and Supplementary Fig. S5). These results suggest that *Se13* might function in the maintenance of the expression amplitudes of the circadian clock oscillator, and that the declined amplitudes of internal clock genes are the main cause of the reduced expression of *Hd1* in X61.

Relationships between the *Se13* locus and the *Hd1* and *Ghd7* loci.

Expression analysis showed that loss-of-function of the *Se13* gene affected the expression levels of *Hd1* and *Ghd7* particularly at 25 DAS. We investigated the relationship between the *Se13* locus and the *Hd1* and *Ghd7* loci using double mutants (*se13hd1*, *se13ghd7*). Days to flowering (DTF) increased in the genotype of *Se13hd1*, but not in the genotype of *se13hd1*. The *se13* gene prevented *ghd7* from decreasing DTF; in the presence of *Se13*, however, *ghd7* greatly

increased DTF. The *hd1ghd7* double-deficient mutants, however, did not flower at the same time as the *se13* recessive lines. These observations clearly demonstrate that, under LD, *Se13* is involved in a genetic photoperiodic flowering pathway that includes *Hd1* and *Ghd7* (Fig. 6).

Discussion

In the present study, we successfully verified that *se13* in the extremely early flowering mutant X61 is a nonsense mutant gene of *OsHY2* encoding phytochromobilin (PΦB) synthase, and that X61 is almost, but not completely, insensitive to red-light signals, as determined through a complementation test followed by spectrometric and photomorphogenic analyses. Comparison of the expression profiles between WT and X61 suggests that the reduction of phytochrome-mediated light signals contributes to decrease the expressions of major photoperiod sensitive genes, *Ghd7* and *Hd1* due to the declined amplitudes of internal clock genes, resulting to early flowering under long day condition.

In rice, phytochrome-mediated light signals play critical roles in controlling flowering time. The rice genome harbors three phytochrome molecules, *PhyA*, *PhyB*, and *PhyC*, and the presence of *PhyB* and *PhyC* is essential for the inhibition of flowering under LD conditions⁴⁹. Also, the presence of the homo-dimer *PhyA* and the hetero-dimer *PhyB-PhyC* is assumed to be indispensable for the expression of photoperiod sensitivity. In a rice nonfunctional mutant for the *Se5* locus encoding heme oxygenase in the phytochrome-chromophore biosynthesis pathway, *Hd1* expression level decreased under LD conditions at 28 DAS⁴⁰, indicating that *Hd1* is regulated by phytochrome-mediated light signals. Moreover, *Ghd7* is a flowering time repressor whose expression is determined by the coincidence of the timing of gating and phytochrome-mediated light signals¹⁹. In the present study, the diurnal expression of *Hd1* in X61 decreased under LD at 25 and 28 DAS (Fig. 4c and d), while those at 18 and 22 DAS were not different between WT and X61 (Fig. 4a and b). On the other hand, the *Ghd7* expression at 25 DAS was reduced from the dusk to the beginning of the next light period, and that at 28 DAS was markedly reduced (Fig. 4c and d). In addition, we found that the *Se13* locus interacts with the *Hd1* and *Ghd7* loci, affecting flowering time under LD (Fig. 6). These results indicate that the inactivation of phytochromes caused by the deficiency of PΦB synthase brings about reduced expressions of *Hd1* and *Ghd7* along with the developmental growth. Interestingly, although the *Ghd7* expressions at 18 and 22 DAS were not different between WT and X61, that at 18 DAS was lower than that at 22 DAS (Fig. 4a and b). Matsubara et al.¹² reported that *Ghd7* expression is developmentally regulated: the gene activity is highest over the two weeks after germination and then gradually decreases to a basal level. Therefore, the up-regulation of *Ghd7* at 22

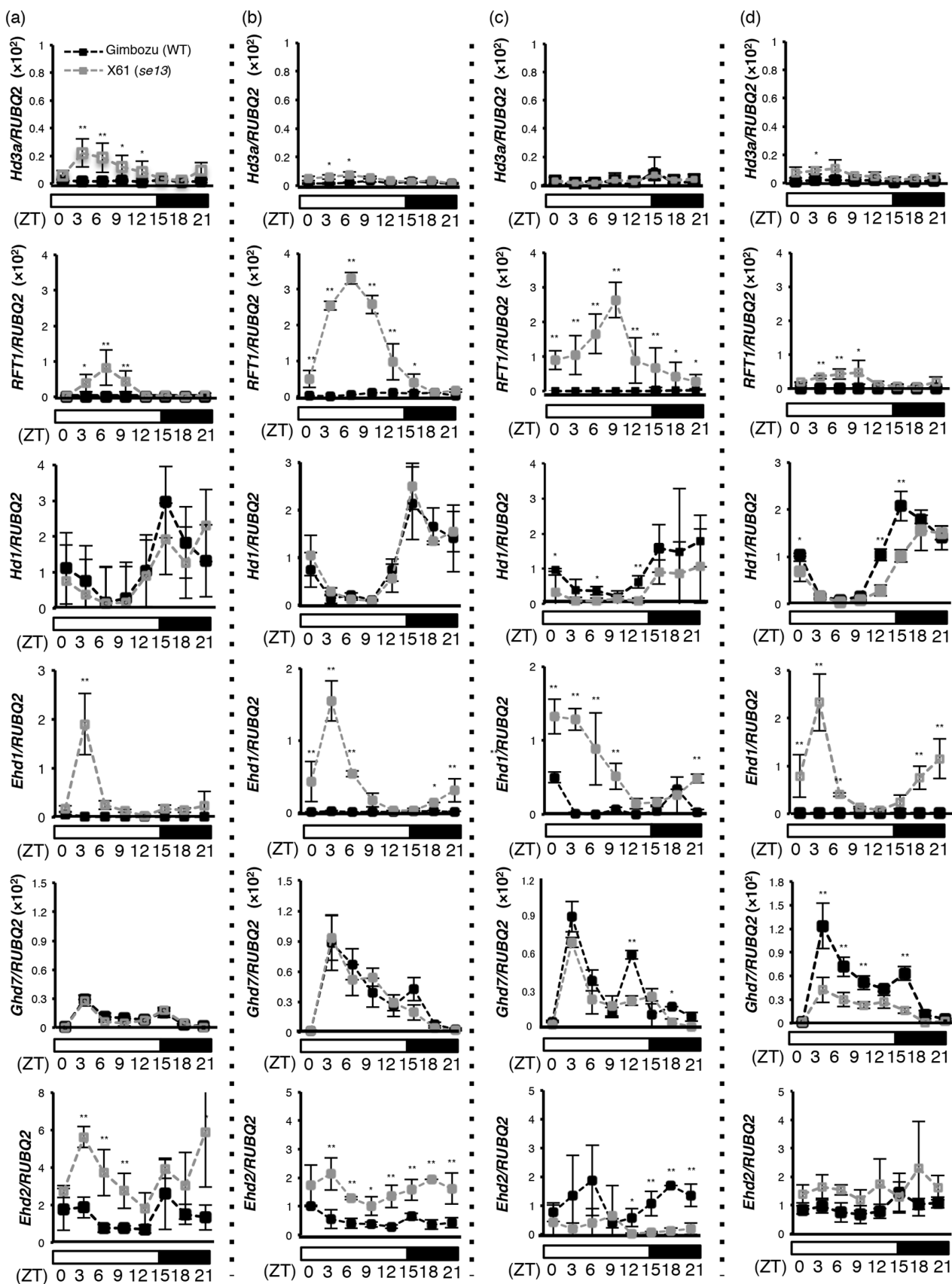


Figure 4 | Diurnal expressions of flowering time genes at 18, 22, 25 and 28 DAS. Expression profiles (a) at 18 DAS (b) at 22 DAS (c) at 25 DAS (d) at 28 DAS. Y-axis indicates investigated gene expression levels. Plants were grown under LD conditions. Transcription levels were observed every 3 h. Measurements were repeated three times using three biological replicates. Average values \pm s.d. are shown. RUBQ2 is a ubiquitin gene used for the normalization of expression levels. LD, long day. ZT, Zeitgeber time (ZT 0: beginning of light period). White and black bars indicate light and dark periods respectively. A two-tailed Student's t-test tested the difference between two means: ** $0.05 < P < 0.01$; * $P < 0.01$.

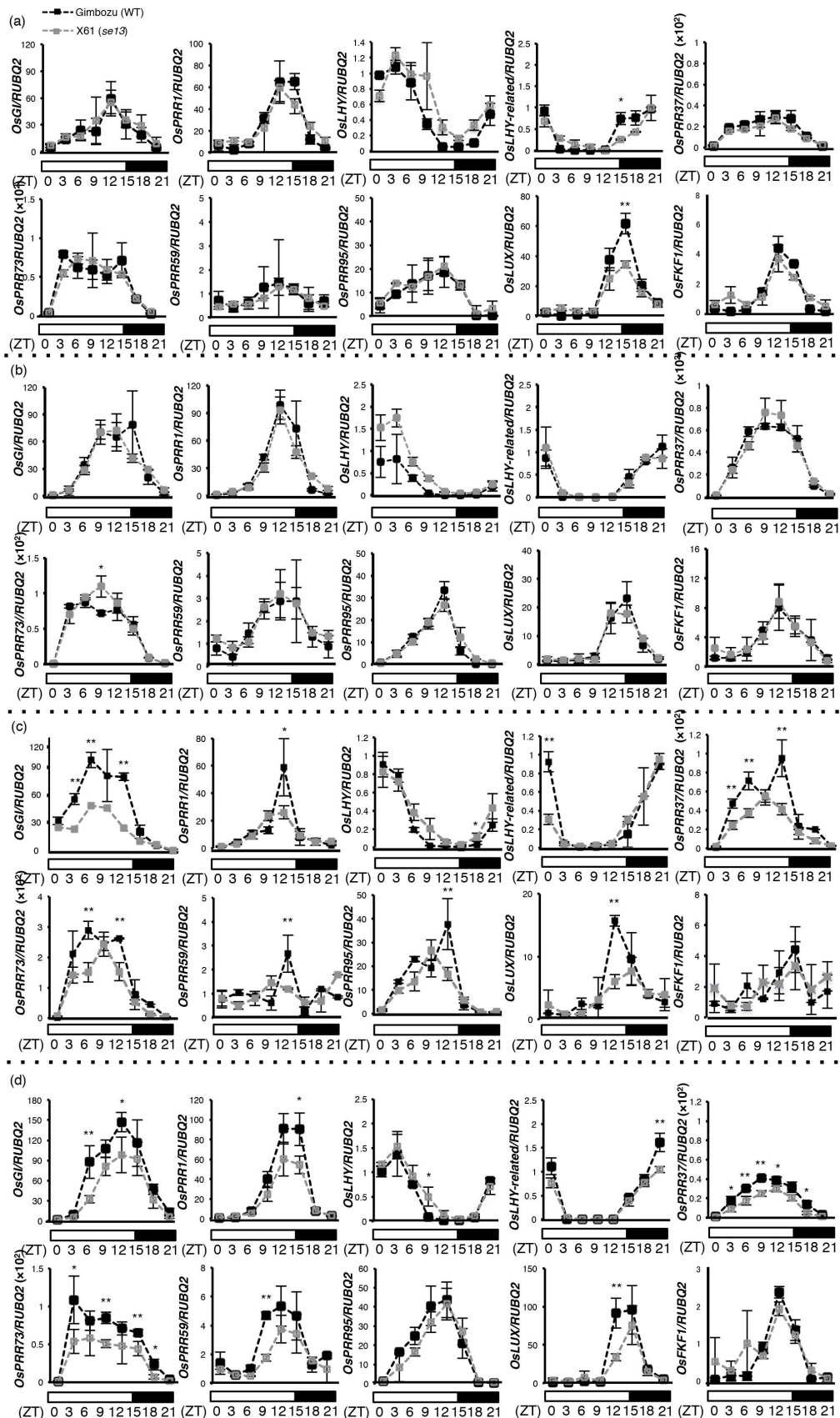


Figure 5 | Diurnal expressions of circadian clock genes at 18, 22, 25 and 28 DAS. Expression profiles (a) at 18 DAS (b) at 22 DAS (c) at 25 DAS (d) at 28 DAS. Y-axis indicates investigated gene expression levels. Plants were grown under LD (14.5-h light/9.5-h dark) conditions. Transcription levels were observed every 3 h. Measurements were repeated three times using three biological replicates. Average values \pm s.d. are shown. RUBQ2 is a ubiquitin gene used for the normalization of expression levels. LD, long day. ZT, Zeitgeber time (ZT 0: beginning of light period). White and black bars indicate light and dark periods respectively. A two-tailed Student's t-test tested the difference between two means: **0.05 < P < 0.01; *P < 0.01.

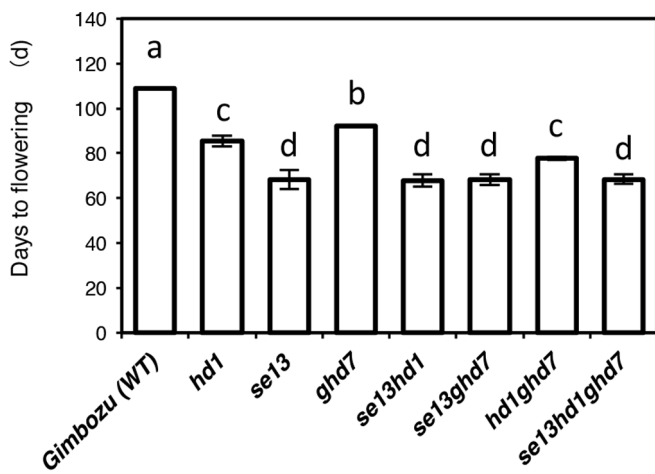


Figure 6 | Effect of the *se13* mutant gene on flowering time and its effect in combination with non-functional *Ghd7* or *Hd1* alleles observed under LD conditions. Mean values of 300 plants and error bars representing \pm s.d. are shown. Means followed by different letters are significantly different from that of WT [$P < 0.05$ according to Tukey's honest significant difference test (a-d)].

DAS is consistent with previous report. However, we do not have a clear answer to the question of why significant differences in *Ghd7* expression were not seen between X61 and WT at 18 and 22 DAS. It is considered that a weak light signal might be enough to induce the *Ghd7* expression, or that other unknown factors associated with the circadian clock might be involved in its up-regulation. This question remains to be explored in future studies.

In *Arabidopsis*, the amplitude of rhythmic oscillation/luminescence (*pCCA1::LUC2*) in the phytochrome null mutant (*phyABCDE*), which was completely insensitive to red-light signals, was greatly reduced compared to that in the WT³⁶. To maintain the oscillation of clock genes, *ELF3* integrates phytochrome-mediated light (red light) signals by binding to the *PRR9* promoter sequence in a *LUX*-dependent manner³⁷. Although Nagano et al.³⁰ indicates that not all clock components were conserved between *Arabidopsis* and rice, some clock-associated genes, such as *OsCCA1* and the *OsPRR*-series including *OsTOC1/OsPRR1*, *OsZTLs* and *OsLUX*, as well as *OsGI* are highly conserved²⁹. At 25 and 28 DAS, the peak expression levels of *OsGI* and most of the *OsPRR* gene series were decreased in X61, while those at 18 and 22 DAS were not different between WT and X61 (Fig. 5). Hayama et al.¹⁴, Shibaya et al.⁵² and Lin et al.⁵³ reported that *OsGI* and *OsPRR37* (*Hd2*) regulate *Hd1* and *Ghd7* expressions, respectively. Given this along with the expression profiles of *Hd1* and *Ghd7*, we conclude that the phytochrome-mediated light signals are essential for the amplitude of the normal circadian oscillation, and that the decreased amplitudes of *OsGI* and *OsPRR37* are the major causes of the loss of photoperiod sensitivity in X61. However, the diurnal expression peak of *OsGI* in WT at 25 DAS seemed to be specifically 6 h earlier than those at the other three time points (Fig. 5). It is unclear why the peak timing of *OsGI* is around ZT6 only at 25 DAS, or whether this peak shift is biologically significant event. In this study, however, we found the significant down-regulation of *OsGI* expression at 25 and 28 DAS in X61. Although our current understanding of the circadian clock in rice is not sufficient to explain how the clock is regulated, we regard the down-regulation of the peak expression levels of *OsGI* and most of the *OsPRR* gene series as a trigger for the down-regulation of *Hd1* and *Ghd7*. Further analyses are necessary to resolve this matter.

We demonstrated a distinct differences in gene expression profiles based on phytochrome-mediated light signals between the earlier time points (18 DAS and 22 DAS) and the later time points (25

DAS and 28 DAS), establishing the earlier time points in one developmental stage and the later time points in another. Daylength transfer experiments showed that the first and second developmental stages were likely to correspond with the duration of BVP and PSP, respectively. In a narrow interpretation, the duration of PSP is defined as an effective growth stage of long-day dependent floral repression, while the duration of BVP is defined as a non-effective growth stage of long-day dependent floral repression. Therefore, the physiological differences in the responsiveness to phytochrome-mediated light signal might contribute to the differences of developmental stages (Fig. 7). In addition, the expression amplitudes of circadian clock genes were clearly different between in the BVP and the PSP (Fig. 5). These results suggest that the contribution of phytochrome (red light) signals to the circadian clock oscillations might be, along with developmental growth, the main means by which the

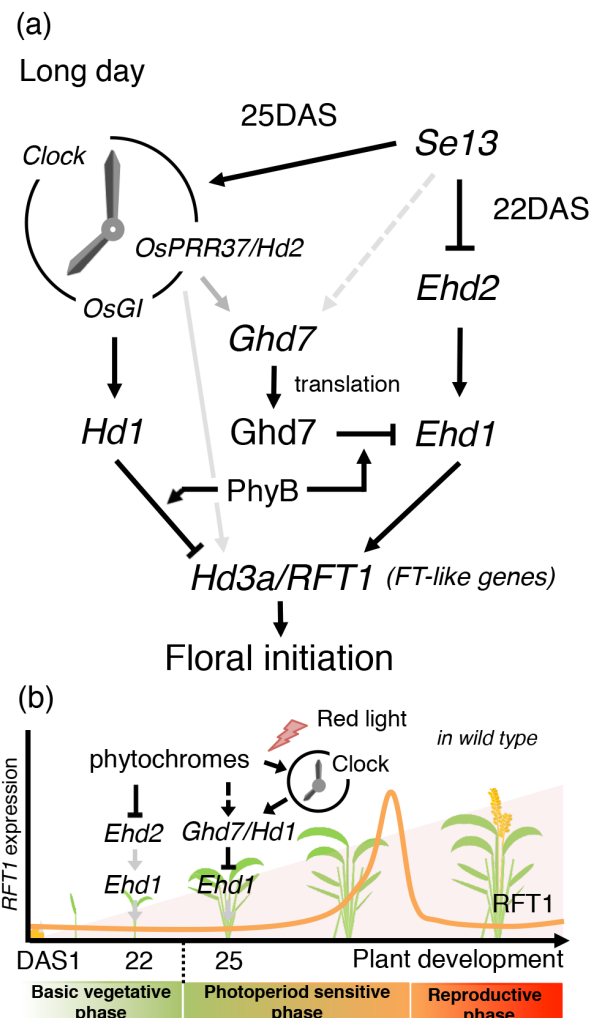


Figure 7 | A proposed model for the photoperiodic control of rice flowering in long day conditions. (a) *Se13*, which encodes phytochromobilin synthase, represses *Ehd2* expression in BVP and activates *Ghd7* and *Hd1* expressions via the circadian genes *OsPRR37/Hd2* and *OsGI* during PSP, respectively. (b) Under LD conditions, expressions of *Ehd1* and *RFT1* are suppressed until a late stage of development (around 70 DAS)^{48,70}. This is caused by the suppression of *Ehd2* expression during the early developmental stage corresponding to BVP. After developmental phase transition to PSP, the expressions of *Ehd1* and *RFT1* are suppressed by *Hd1* and *Ghd7* expressions mediated by the circadian clock. Thus, *Se13* delays flowering in rice under LD conditions. Pointed arrows indicate the upregulation of a gene; blunt-ended arrows indicate the downregulation of a gene.



long-day dependent floral repression is acquired during development (Fig. 7). Further experiments are necessary to clarify the developmental acquisition of the floral repression.

It is noteworthy that at 18 and 22 DAS, the expression of *RFT1* in X61 was upregulated despite the high expressions of *Ghd7* and *Hd1* (Fig. 4a and b). According to previous reports, *Ghd7* and *Hd1* proteins require *PhyB* to exercise their flowering-inhibiting functions^{50,54}. It is therefore considered that in X61, *Ghd7* and *Hd1* proteins were not able to produce their usual effect due to the lack of sufficient phytochrome-mediated light signals. Furthermore, the expressions of *Ehd2* and *Ehd1* were highly upregulated in X61 (Fig. 4a and b). Since *Ehd2* (*RID1*, *OsID1*) is a positive regulator of *Ehd1*^{16–18}, we concluded that the upregulation of *RFT1* in X61 at 18 and 22 DAS is caused by *Ehd1* expression promoted by *Ehd2*, in addition to the light signal's being of insufficient strength to mediate *Ghd7* and *Hd1* proteins. Although previous studies have demonstrated that *Ehd2* (*RID1*, *OsID1*) mRNA is more abundant in younger leaves than in older ones, obvious up-regulations at 18 and 22 DAS were observed in X61 leaves, which were completely opened (Fig. 4a and b). At 25 and 28 DAS, *Ehd2* expression in X61 was not changed compared to WT during the daytime (Fig. 4c and d). These findings indicate that the reductions in older leaves at 18 and 22 DAS are regulated by phytochrome-mediated light signals. Future studies will help to clarify why the changes in expression profiles in *Ehd2* (*RID1*, *OsID1*) are associated with the transition between developmental phases.

In the present study, X61 showed normal development until seed maturity, although the *Se13*-silenced plants were lethal (Fig. 2a). In *Escherichia coli* and *Arabidopsis*, mutants deficient in ferrochelatase (FC), which catalyzes Proto-to-heme conversion, became lethal due to over-accumulation of Proto^{55,56}. However, Proto was significantly accumulated in both *Se13*-silenced lines and X61. Since X61 shows normal development until seed maturity, Proto accumulation is considered not to be a direct cause of the lethality of the *Se13*-silenced lines (Fig. 3i). Instead, the excessive reduction in the amount of chlorophylls in *Se13*-silenced lines is the most likely cause of the lethality although there were no significant reductions in the amounts of Mg-Proto and Mg-ProtoMe in *Se13*-silenced lines compared to WT. Red light is known to promote the greening process in etiolated seedlings by dramatically accumulating the protochlorophyllide oxidoreductase, *PorA* and *PorB*^{57,58}, which catalyze the conversion of protochlorophyllide into chlorophylls, suggesting that *PorA* and *PorB* might not be accumulated in *Se13*-silenced lines. Moreover, under white light, plant height and coleoptile elongation of *Se13*-silenced seedlings were not inhibited; rather, they were comparable to those of WT seedlings grown in the dark (Fig. 2a, d). It is well known that *PhyB* plays a major role in the inhibition of seedling elongation via red light signaling⁴⁹. These results indicate that *Se13*-silenced plants completely lose red light photosensory capabilities. In the heme branch of the phytochrome-chromophore biosynthesis pathway of *Arabidopsis*, there are two enzymatic reactions mediated by heme oxygenase (HY1) and PΦB synthase (HY2) that are involved in phytochromobilin biosynthesis in the plastid^{43,44}. In higher plants, heme oxygenase is governed by small gene families and gene repeats⁵⁹, whereas PΦB synthase is governed by a single gene, in contrast to the significance of the phytochrome signals (SALAD-DB, <http://salad.dna.affrc.go.jp> and ref. 43). The *pew1* and *pew2* (HY1 and HY2 orthologs) double mutants in *N. plumbaginifolia* showed lethality at an early stage of development⁶⁰. Thus, the normal metabolic process of phytochromobilin biosynthesis seems to be indispensable to the growth of the plant.

Growth retardation in the HY2-deficient *Arabidopsis* mutants is generally less than that in HY1-deficient mutants⁶¹. It is known that PΦB synthase is highly conserved among many plant species; in addition, all the known PΦB synthase mutants are leaky, and a small deletion(s) and a simple base change(s) in an exon seldom leads to

severe growth retardation⁶⁰. HY2 is categorized as one of the ferredoxin (Fd)-dependent bilin reductases (FDBRs)⁴³, which requires ferredoxins (FDs) as electron donors for double bond reductions, and the PΦB synthesis step was catalyzed most efficiently by an HY2: BV-AtFd2 heterodimeric complex⁶³. Site-directed mutagenesis analyses in the predicted FDs docking site of HY2 residues demonstrated that all mutants still retained the ability to bind BV⁶³. Using 3'-RACE PCR on the *Se13* transcripts, we identified six different RACE products (Supplementary Fig. S1a and b). Although X61 harbors a 1-bp insertion in exon 1 of *OsHY2*, other transcript variants, such as transcript ζ -type, might redundantly function as counterparts in forming the OsHY2: BV-Fd heterodimeric complex. This may be the reason why X61 retains the ability to respond to red and far-red light unless it disturbs the formation of the OsHY2: BV-Fd heterodimeric complex. On the other hand, we used the common sequences of six RACE fragments to create the *Se13*-silenced plants. It is therefore considered that *Se13*-silenced transgenic plants could be obtained through the potent disruption of translation of truncated functional proteins (Supplementary Fig S1a). Thus, we postulate that complete inactivation of red/far-red perception due to inability to absorb red light because of a complete deficiency of phytochromobilin (PΦB) synthesis caused the severe reduction in chlorophyll content; consequently, the *Se13*-strongly-silenced plants exhibited serious damages (lethality) on plants.

It is well known that rice plants do not respond to the photoperiod during BVP^{1,2}. Many previous studies have identified a large number of flowering time genes and demonstrated that photoperiod sensitivity is determined by a coincidence of internal clock oscillations and external light signals. However, there have not been any clear answers as to how the clock and light signals are integrated with the mechanism responsible for the developmental acquisition of photoperiod sensitivity. Although it remains unknown why rice plants do not respond to the photoperiod during BVP, the phenomena reported here is expected to help us uncover how the light signaling (red light) adjusts circadian oscillation and regulates the photoperiodic repression of flowering time under long day condition during PSP. Furthermore, this developmental transition corresponds to sexual maturation in most species, including insects, birds and mammals. Thus, our findings will also provide valuable information toward understanding sexual maturation and other photo-period-dependent developmental processes, such as migration, hibernation, sexual behavior, and resizing of sexual organs.

Methods

Plant materials. The extremely early flowering time mutant line X61 and its original variety Gimbozu (WT) were used. Gimbozu is a *japonica* rice variety that had been cultivated in Japan at least since the 1940s and perhaps for as long as 100 years. X61 is a mutant line that was induced by X-ray irradiation of WT seeds⁴¹. In addition, *se5* and *se5se13* were used. *se5* is an extremely early flowering time mutant line that was induced by gamma-irradiation of the *japonica* variety Norin-8, which is genetically close to WT³⁹, whereas *se5se13* is a double mutant line that was developed as a cross between X61 and *se5*. The single mutant line, *hd1*, harbors a photoperiod-insensitive allele with the transposable element *mping* inserted at the intron region of *Hd1*⁶. The single mutant line, *ghd7* harbors a photoperiod-insensitive allele at the *E1* locus, which is identical to the *Ghd7* locus³³. *se13hd1* and *se13ghd7* are double mutant lines that were developed as crosses between X61 and *hd1*, and between X61 and *ghd7*, respectively.

Growth conditions. Plants were grown in growth cabinets with environmental controllers (LPH-240SP; Nippon Medical & Chemical Instruments Co., Ltd, Osaka, Japan) at 70% humidity and 400-ppm CO₂ concentrations under either SD conditions, consisting of daily cycles of 10 h light at 30°C and 14 h dark at 25°C, or under LD conditions, consisting of 14.5 h light and 9.5 h dark. Fluorescent white light tubes (400–700 nm, 100 $\mu\text{mol}\cdot\text{m}^{-2}\cdot\text{s}^{-1}$) were used as the artificial light source.

Photoperiodic transfer treatment. According to the analytical model of Ellis et al.⁴⁷ and Nishida et al.¹⁹, we performed a non-linear regression analysis using a data set obtained through photoperiodic transfer treatments with Sigma Plot software, ver. 12 (Cranes Software International Limited, India). We set two daylength conditions: the short daylength (SD) was 10 h, and the long daylength (LD) was 24 h. Germinated seeds were sown on field soil in 5-cm square pots and covered with granulated soil.



Seedlings were thinned to four plants per pot at 14 DAS. The plants were grown with daily cycles of 10 h of light at 30°C and 14 h of dark at 25°C for the SD condition, or continuous light at 30°C for the LD condition. Fluorescent white light tubes (400–700 nm, 100 $\mu\text{mol}\cdot\text{m}^{-2}\cdot\text{s}^{-1}$) were used as the artificial light source. Thirteen pots for each line were initially kept under LD conditions. Seven days after sowing, one pot per line was transferred to the SD conditions. Once a pot had been transferred, it was kept under SD conditions until flowering. One pot per lines was transferred at each of the following time points: 0, 7, 14, 21, 28, 35, 42, 49, 56, 63, 70, and 77 DAS.

Plasmid construction and transformation. The full-length cDNA was isolated by PCR using the primer pair to conjugate *Bam*H1 and *Sac*I sites at the 5' and 3' ends respectively, with primer pair forward, 5'-GGGAGAGAGCATGAGCAG-CGGCGCGT-3', and reverse, 5'- AGCGAACATTTACTGTGCTTCGGCAT-3'. PCR products were sub-cloned into a pBluescript SKII+ vector and were introduced into the pMLH7133 plant expression vector⁶⁴. The *Agrobacterium tumefaciens* (EHA101 strain)-mediated method was used for the transformation of the full-length cDNA of *Se13* into X61 for the complementation test.

For the silencing of *Se13*, 3'UTR of *Se13* was isolated by PCR using the primer pair forward, 5'-CACCTACGCCGTGATGATGGGTCAAG-3', and reverse, 5'-AAGAGGATTGATCAGGCCGAAAGGCG-3'. The PCR products were sub-cloned into pENTR/D-TOPO cloning vector (Life Technologies Inc., Carlsbad, CA, USA) and were introduced into the pANDA vector by means of an LR clonase reaction⁶⁵. Then, the *Agrobacterium tumefaciens* (LBA4404 strain)-mediated method⁶² was used for the transformation of the 3'UTR of *Se13* into the variety *Oryza sativa* japonica cv Nipponbare which is genetically similar to Gimbozu.

High-throughput quantitative RT-PCR (qPCR). Total RNA was isolated with TriPure Isolation Reagent (Roche, Ltd., Basel, Switzerland) and treated with DNase I (Takara Bio Inc., Otsu, Japan). Precisely 1.5 μg total RNA was used for first-strand cDNA synthesis using the Transcripter Universal cDNA Master with random primer (Roche Ltd.). cDNA that had been preamplified (for 18 cycles) using a TaqMan preamp master mix kit (Life Technologies Inc.) was used for qPCR after five-fold dilution with TE buffer (Teknova Inc., Hollister, CA). Precisely 10 nL of pre-amplified cDNA per sample was used for the quantitative analysis of gene expression performed with TaqMan Universal PCR Master Mix (Applied Biosystems Inc., Foster City, CA, USA) using gene-specific primers and probes. The melting curve analyses were performed in advance to quantify the PCR efficiency and to test correlations between different regular qPCR. All the samples attained the critical value of $R > 0.97$ and $0.9 < \text{slope} < 1.1$. Forty-eight gene assays and cDNA samples were loaded into separate wells on a 48 \times 48 gene expression chip (48.48 Fluidigm Dynamic Arrays; Fluidigm Corp., South San Francisco, CA, USA). The qPCR was run on the Biomark HD system (Fluidigm Corp.; 10 min at 95°C for activation of the hot-start enzyme, followed by 40 cycles of denaturation at 95°C for 15 s, annealing at 70°C for 5 s, and elongation at 60°C for 60 s). Relative RNA expression for each gene in a sample was standardized to the endogenous housekeeping gene rice ubiquitin (*RUBQ2*) and was calculated according to the delta-delta CT method⁶⁶. All assays were replicated three times using three different plant samples.

Spectroscopic measurements of Phytochrome. Measurements were taken according to methods described previously^{39,45}. Phytochromes were extracted from the shoot of seven-day-old etiolated seedlings and partially purified with an ammonium sulfate precipitation as described in the literature³⁹. The absorption difference spectra of phytochromes in the extract were measured with a U3310 spectrophotometer (Hitachi Technologies, Tokyo, Japan). All difference spectra were obtained by averaging the results of three photoconversions by red and successive far-red irradiations. Saturating red (660 nm) or far-red (730 nm) light was supplied from the excitation light of a RF-5300PC fluorescence spectrophotometer (Shimadzu Co., Ltd., Kyoto, Japan) using a light guide. All procedures were performed under a dim green safety light.

Measurement of chlorophyll content. Samples of fresh leaves were taken from two-week-old seedlings. At least two seedlings were sampled in each replication, and the samplings were conducted three times for measurement. Extraction and measurement of chlorophyll a and b content was performed according to methods described previously⁶⁶. The absorption difference spectra of chrolophyll in the extracts were measured with a spectrophotometer (Biospec-1600; Shimadzu Co., Ltd.).

Quantification of ProtoIX, MgProto, and MgProtoMe. Plant material (50–100 mg) was weighed and frozen in liquid nitrogen, then ground using a 2-mL sample tube grinding apparatus (Yasui-kikai Corp., Osaka, Japan). The powdered samples were suspended with 0.1 mL of acetone chilled at –20°C and centrifuged at 10,000 $\times g$ (4°C) for 10 min. The residues were re-extracted with 0.1 mL of acetone chilled at –20°C and repeated immediately. After combining the supernatants, the volume was measured and stored in darkness at 4°C until HPLC analysis. Pigments were separated on a reverse phase C18 column (150 \times 2.1 mm; 4- μm particle diameter Nova-Pak®; Waters, Milford, MA, USA) using an HPLC system (LC-VP; Shimadzu Co. Ltd.) equipped with a fluorescence detector (RF-10AXL; Shimadzu Co. Ltd.). Standard curves were constructed according to the authentic standards purchased from Frontier Scientific Inc. (Logan, UT, USA). HPLC conditions were performed according to methods described previously⁶⁷.

- Vergara, B. S. & Chang, T. T. *The flowering response of the rice plant to photoperiod: A review of the literature*. (The International Rice Research Institute, Los Banos, 1985).
- Nishida, H. *et al.* Analysis of tester lines for rice (*Oryza sativa* L.) heading-time genes using reciprocal photoperiodic transfer treatments. *Ann. Bot.* **88**, 527–536 (2001).
- Kojima, S. *et al.* Hd3a, a rice ortholog of the *Arabidopsis* *FT* gene, promotes transition to flowering downstream of Hd1 under short-day conditions. *Plant Cell Physiol.* **43**, 1096–1105 (2002).
- Hayama, R. *et al.* Adaptation of photoperiodic control pathways produces short-day flowering in rice. *Nature* **422**, 719–722 (2003).
- Tamaki, S. *et al.* Hd3a protein is a mobile flowering signal in rice. *Science* **316**, 1033–1036 (2007).
- Yano, M. *et al.* Hd1, a major photoperiod sensitivity quantitative trait locus in rice, is closely related to the *Arabidopsis* flowering time gene CONSTANS. *Plant Cell* **12**, 2473–2484 (2000).
- Doi, K. *et al.* Hd1, a B-type response regulator in rice, confers short-day promotion of flowering and controls FT-like gene expression independently of Hd1. *Genes Dev.* **18**, 926–936 (2004).
- Lee, S. *et al.* Functional analyses of the flowering time gene OsMADS50, the putative suppressor of overexpression of CO 1/Agamous-like 20 (SOC1/AGL20) ortholog in rice. *Plant J.* **38**, 754–764 (2004).
- Kim, S. *et al.* OsMADS51 is a short-day flowering promoter that functions upstream of Hd1, OsMADS14, and Hd3a. *Plant Physiol.* **145**, 1484–1494 (2007).
- Ryu, C.-H. *et al.* OsMADS50 and OsMADS56 function antagonistically in regulating long day (LD)-dependent flowering in rice. *Plant Cell Environ.* **32**, 1412–1427 (2009).
- Xue, W. *et al.* Natural variation in Ghd7 is an important regulator of heading date and yield potential in rice. *Nat. Genet.* **40**, 761–767 (2008).
- Matsubara, K. *et al.* Ehd3, encoding a plant homeodomain finger-containing protein, is a critical promoter of rice flowering. *Plant J.* **66**, 603–612 (2011).
- Lee, Y.-S. *et al.* OsCOL4 is a constitutive flowering repressor upstream of Ehd1 and downstream of OsPhyB. *Plant J.* **63**, 18–30 (2010).
- Hayama, R., Izawa, T. & Shimamoto, K. Isolation of rice genes possibly involved in the photoperiodic control of flowering by a fluorescent differential display method. *Plant Cell Physiol.* **43**, 494–504 (2002).
- Izawa, T. *et al.* Os-GIGANTEA confers robust diurnal rhythms on the global transcriptome of rice in the field. *Plant Cell* **23**, 1741–1755 (2011).
- Matsubara, K. *et al.* Ehd2, a rice ortholog of the maize INDETERMINATE1 gene, promotes flowering by up-regulating Ehd1. *Plant Physiol.* **148**, 1425–1435 (2008).
- Wu, C. *et al.* RID1, encoding a Cys2/His2-type zinc finger transcription factor, acts as a master switch from vegetative to floral development in rice. *Proc. Natl. Acad. Sci. U.S.A.* **105**, 12915–12920 (2008).
- Park, S. *et al.* Rice Indeterminate 1 (OsId1) is necessary for the expression of Ehd1 (Early heading date 1) regardless of photoperiod. *Plant J.* **56**, 1018–1029 (2008).
- Ogiso, E. *et al.* The role of casein kinase II in flowering time regulation has diversified during evolution. *Plant Physiol.* **152**, 808–820 (2010).
- Itoh, H., Nonoue, Y., Yano, M. & Izawa, T. A pair of floral regulators sets critical day length for Hd3a florigen expression in rice. *Nat. Genet.* **42**, 635–638 (2010).
- Strayer, C. *et al.* Cloning of the *Arabidopsis* clock gene TOC1, an autoregulatory response regulator homolog. *Science* **289**, 768–771 (2000).
- Schaffer, R. *et al.* The late elongated hypocotyl mutation of *Arabidopsis* disrupts circadian rhythms and the photoperiodic control of flowering. *Cell* **93**, 1219–1229 (1998).
- Wang, Z. & Tobin, E. Constitutive expression of the circadian clock associated 1 (CCA1) gene disrupts circadian rhythms and suppresses its own expression. *Cell* **93**, 1207–1217 (1998).
- Alabadi, D. *et al.* Reciprocal regulation between TOC1 and LHY/CCA1 within the *Arabidopsis* circadian clock. *Science* **293**, 880–883 (2001).
- Locke, J. *et al.* Experimental validation of a predicted feedback loop in the multi-oscillator clock of *Arabidopsis thaliana*. *Mol. Syst. Biol.* **2**, 59 (2006).
- Zeilinger, M. *et al.* A novel computational model of the circadian clock in *Arabidopsis* that incorporates PRR7 and PRR9. *Mol. Syst. Biol.* **2**, 58 (2006).
- Fowler, S. *et al.* Gigantea: A circadian clock-controlled gene that regulates photoperiodic flowering in *Arabidopsis* and encodes a protein with several possible membrane-spanning domains. *EMBO J.* **18**, 4679–4688 (1999).
- Makino, S. *et al.* The APRR1/TOC1 quintet implicated in circadian rhythms of *Arabidopsis thaliana*: I. Characterization with APRR1-overexpressing plants. *Plant Cell Physiol.* **43**, 58–69 (2002).
- Murakami, M., Tago, Y., Yamashino, T. & Mizuno, T. Comparative overviews of clock-associated genes of *Arabidopsis thaliana* and *Oryza sativa*. *Plant Cell Physiol.* **48**, 110–121 (2007).
- Nagano, A. *et al.* Deciphering and prediction of transcriptome dynamics under fluctuating field conditions. *Cell* **151**, 1358–1369 (2012).
- Koo, B.-H. *et al.* Natural variation in OsPRR37 regulates heading date and contributes to rice cultivation at a wide range of latitudes. *Mol. Plant.* **6** 1877–1888 (2013).
- Yuan, Q. *et al.* Identification of a novel gene ef7 conferring an extremely long basic vegetative growth phase in rice. *Theor. Appl. Genet.* **119**, 675–684 (2009).
- Saito, H. *et al.* Ef7 encodes an ELF3-like protein and promotes rice flowering by negatively regulating the floral repressor gene Ghd7 under both short- and long-day conditions. *Plant Cell Physiol.* **53**, 717–728 (2012).



34. Matsubara, K. *et al.* Natural variation in Hd17, a homolog of *Arabidopsis* ELF3 that is involved in rice photoperiodic flowering. *Plant Cell Physiol.* **53**, 709–716 (2012).
35. Yang, Y. *et al.* OsELF3 is involved in circadian clock regulation for promoting flowering under long-day conditions in rice. *Mol. Plant* **6**, 202–215 (2013).
36. Hu, W. *et al.* Unanticipated regulatory roles for *Arabidopsis* phytochromes revealed by null mutant analysis. *Proc. Natl. Acad. Sci. U S A* **110**, 1542–1547 (2013).
37. Herrero, E. *et al.* EARLY FLOWERING4 recruitment of EARLY FLOWERING in the nucleus sustains the *Arabidopsis* circadian clock. *Plant Cell* **24**, 428–43 (2012).
38. Takano, M. *et al.* Phytochromes are the sole photoreceptors for perceiving red/far-red light in rice. *Proc. Natl. Acad. Sci. U S A* **106**, 14705–14710 (2009).
39. Izawa, T. *et al.* Phytochromes confer the photoperiodic control of flowering in rice (a short-day plant). *Plant J.* **22**, 391–399 (2000).
40. Andrés, F., Galbraith, D., Talón, M. & Domingo, C. Analysis of photoperiod sensitivity 5 sheds light on the role of phytochromes in photoperiodic flowering in rice. *Plant Physiol.* **151**, 681–690 (2009).
41. Saito, H. *et al.* Complete loss of photoperiodic response in the rice mutant line X61 is caused by deficiency of phytochrome chromophore biosynthesis gene. *Theor. Appl. Genet.* **122**, 109–118 (2011).
42. Komari, T. *et al.* Vectors carrying two separate T-DNA for co-transformation of higher plants mediated by *Agrobacterium tumefaciens* and segregation of transformants free from selection markers. *Plant J.* **10**, 165–174 (1996).
43. Kohchi, T. *et al.* The *Arabidopsis* HY2 gene encodes phytochromobilin synthase, a ferredoxin-dependent biliverdin reductase. *Plant Cell* **13**, 425–436 (2001).
44. Muramoto, T. *et al.* The *Arabidopsis* photomorphogenic mutant hyl is deficient in phytochrome chromophore biosynthesis as a result of a mutation in a plastid heme oxygenase. *Plant Cell* **11**, 335–48 (1999).
45. Pjon, C. & Furuya, M. Phytochrome action in *Oryza sativa* L. II. The spectrophotometric versus the physiological status of phytochrome in coleoptiles. *Planta* **81**, 303–313 (1968).
46. Miki, D. & Shimamoto, K. Simple RNAi vectors for stable and transient suppression of gene function in rice. *Plant Cell Physiol.* **45**, 490–495 (2004).
47. Ellis, R., Collinson, S., Hudson, D. & Patefield, W. The analysis of reciprocal transfer experiments to estimate the durations of the photoperiod-sensitive and photoperiod-insensitive phases of plant development: an example in soya bean. *Ann. Bot.* **70**, 87–92 (1992).
48. Komiya, R. *et al.* Hd3a and RFT1 are essential for flowering in rice. *Development* **135**, 767–774 (2008).
49. Takano, M. *et al.* Distinct and cooperative functions of phytochromes A, B, and C in the control of deetiolation and flowering in rice. *Plant Cell* **17**, 3311–3325 (2005).
50. Osugi, A. *et al.* Molecular dissection of the roles of phytochrome in photoperiodic flowering in rice. *Plant Physiol.* **157**, 1128–37 (2011).
51. Fujino, K., Sekiguchi, H. & Kiguchi, T. Identification of an active transposon in intact rice plants. *Mol. Genet. Genomics* **273**, 150–157 (2005).
52. Shibaya, T. *et al.* Genetic interactions involved in the inhibition of heading by heading date QTL, Hd2 in rice under long-day conditions. *Theor. Appl. Genet.* **123**, 1133–1143 (2011).
53. Lin, H., Liang, Z., Sasaki, T. & Yano, M. Fine mapping and characterization of quantitative trait loci Hd4 and Hd5 controlling heading date in rice. *Breeding Sci.* **53**, 51–59 (2003).
54. Ishikawa, R. *et al.* Phytochrome B regulates heading date 1 (Hd1)-mediated expression of rice florigen Hd3a and critical day length in rice. *Mol. Genet. Genomics* **285**, 461–470 (2011).
55. Miyamoto, K. *et al.* Accumulation of protoporphyrin IX in light-sensitive mutants of *Escherichia coli*. *FEBS Letters* **310**, 246–248 (1992).
56. Woodson, J., Perez-Ruiz, J. & Chory, J. Heme synthesis by plastid ferrochelatase I regulates nuclear gene expression in plants. *Curr. Biol.* **21**, 897–903 (2011).
57. Barnes, S. *et al.* Far-red light blocks greening of *Arabidopsis* seedlings via a phytochrome A-mediated change in plastid development. *Plant Cell* **8**, 601–615 (1996).
58. Sperling, U. *et al.* Overexpression of light-dependent PORA or PORB in plants depleted of endogenous POR by far-red light enhances seedling survival in white light and protects against photooxidative damage. *Plant J.* **12**, 649–658 (1997).
59. Davis, S. *et al.* The heme-oxygenase family required for phytochrome chromophore biosynthesis is necessary for proper photomorphogenesis in higher plants. *Plant Physiol.* **126**, 656–669 (2001).
60. Terry, M. J. Phytochrome chromophore-deficient mutants. *Plant Cell Environ.* **20**, 740–745 (1997).
61. Koornneef, M., Rolff, E. & Spruit, C. Genetic control of light-inhibited hypocotyl elongation in *Arabidopsis thaliana* (L.) Heynh. *Z. Pflanzenphysiol.* **100**, 147–160 (1980).
62. Kraepiel, Y., Jullien, M., Cordonnier-Pratt, M. & Pratt, L. Identification of two loci involved in phytochrome expression in *Nicotiana plumbaginifolia* and lethality of the corresponding double mutant. *Mol. Gen. Genet.* **242**, 559–565 (1994).
63. Chiù, F.-Y., Chen, Y.-R. & Tu, S.-L. Electrostatic interaction of phytochromobilin synthase and ferredoxin for biosynthesis of phytochrome chromophore. *J. Biol. Chem.* **285**, 5056–5065 (2010).
64. Mitsuhashi, I. *et al.* Efficient promoter cassettes for enhanced expression of foreign genes in dicotyledonous and monocotyledonous plants. *Plant Cell Physiol.* **37**, 49–59 (1996).
65. Pfaffl, M. A new mathematical model for relative quantification in real-time RT-PCR. *Nuc. Acids Res.* **29**, e45–e45 (2001).
66. Porra, R., Thompson, W. & Kriedemann, P. Determination of accurate extinction coefficients and simultaneous equations for assaying chlorophylls *a* and *b* extracted with four different solvents. *Biochim. Biophys. Acta* **975**, 384–394 (1989).
67. Mochizuki, N. *et al.* The steady-state level of Mg-protoporphyrin IX is not a determinant of plastid-to-nucleus signaling in *Arabidopsis*. *Proc. Natl. Acad. Sci. U S A* **105**, 15184–15189 (2008).
68. Zhang, H. *et al.* Rice chlorina-1 and chlorina-9 encode ChlD and ChlII subunits of Mg-chelatase, a key enzyme for chlorophyll synthesis and chloroplast development. *Plant Mol. Biol.* **62**, 325–337 (2006).
69. Elich, T. & Lagarias, J. Phytochrome chromophore biosynthesis: both 5-aminolevulinic acid and biliverdin overcome inhibition by gabaculine in etiolated *Avena sativa* L. seedlings. *Plant Physiol.* **84**, 304–310 (1987).
70. Itoh, H. & Izawa, T. The coincidence of critical day length recognition for florigen gene expression and floral transition under long-day conditions in rice. *Mol. Plant* **6**, 635–649 (2013).

Acknowledgments

We thank Dr. Takeshi Izawa (NIAS, Japan) for providing the *se5* mutant; Drs. Ko Shimamoto and Daisuke Miki (NAIST, Japan) for providing the pANDA vector; Drs. Seiichi Toki, Hiroaki Saika and Eri Ogiso-Tanaka (NIAS, Japan) for technical support regarding rice transformation; Drs. Kiyokazu Agata and Norito Shibata (Kyoto University, Japan) for providing the BioMARK HD1 qPCR instrument; Dr. Hisashi Miyagawa (Kyoto University, Japan) for providing the HPLC instrument; Dr. Nobuyoshi Mochizuki (Kyoto University, Japan) for providing the Mg-ProtoMe standards and for information on GUN1 and GUN4 prior to publication; and Drs. Akira Kitajima and Tetsuya Nakazaki for supporting the expression analyses.

Author contributions

Y.Y. designed and performed the majority of the experiments. T.Y. and X.Q. conducted the identification and cloning of *Se13*. T.A., N.M. and T.K. performed molecular characterization of *Se13*. H.S., H.N. and Y.O. performed photoperiod transfer treatment and data analysis. H.S., K.Z., H.K. and S.T. conducted spectroscopic measurements of phytochrome. H.I., M.T. and Y.O. provided the X61 plant. Y.Y., H.S., T. Tsukiyama, T. Tanisaka and Y.O. wrote the manuscript. All authors reviewed the manuscript.

Additional information

Supplementary information accompanies this paper at <http://www.nature.com/scientificreports/>

Competing financial interests: The authors declare no competing financial interests.

How to cite this article: Yoshitake, Y. *et al.* The effects of phytochrome-mediated light signals on the developmental acquisition of photoperiod sensitivity in rice. *Sci. Rep.* **5**, 7709; DOI:10.1038/srep07709 (2015).



This work is licensed under a Creative Commons Attribution-NonCommercial-NoDerivs 4.0 International License. The images or other third party material in this article are included in the article's Creative Commons license, unless indicated otherwise in the credit line; if the material is not included under the Creative Commons license, users will need to obtain permission from the license holder in order to reproduce the material. To view a copy of this license, visit <http://creativecommons.org/licenses/by-nc-nd/4.0/>